On the Reversible O_2 Binding of the Fe–Porphyrin Complex

HIROYUKI NAKASHIMA,[1] JUN-YA HASEGAWA,[1] HIROSHI NAKATSUJI,[1,2]
[1]*Department of Synthetic Chemistry and Biological Chemistry, Graduate School of Engineering, Kyoto University, Katsura, Nishikyo-ku, Kyoto 615-8510, Japan*
[2]*Fukui Institute for Fundamental Chemistry, Kyoto University, Takano-Nishihiraki-cho 34-4, Sakyo-ku, Kyoto 606-8103, Japan*

Received 27 January 2005; Accepted 31August 2005
DOI 10.1002/jcc.20339
Published online in Wiley InterScience (www.interscience.wiley.com).

Abstract: Electronic mechanism of the reversible O_2 binding by heme was studied by using Density Functional Theory calculations. The ground state of oxyheme was calculated to be open singlet state [Fe(S =1/2) + O_2(S = 1/2)]. The potential energy surface for singlet state is associative, while that for triplet state is dissociative. Because the ground state of the O_2 + deoxyheme system is triplet in the dissociation limit [Fe(S = 2) + O_2(S = 1)], the O_2 binding process requires relativistic spin-orbit interaction to accomplish the intersystem crossing from triplet to singlet states. Owing to the singlet-triplet crossing, the activation energies for both O_2 binding and dissociation become moderate, and hence reversible. We also found that the deviation of the Fe atom from the porphyrin plane is also important reaction coordinate for O_2 binding. The potential surface is associative/dissociative when the Fe atom locates in-plane/out-of-plane.

 J Comput Chem 27: 426–433, 2006

Key words: reversible O_2 binding; heme; potential energy surface; intersystem crossing

Introduction

Hemoglobin and myoglobin play indispensable roles in the living body: transport and storage of dioxygen. These processes have been studied in detail both theoretically and experimentally.[1–10] Hemoglobin and myoglobin have the same active site, heme (Fe–porphyrin complex), and the tertiary structure of a subunit of hemoglobin is very similar to that of myoglobin. However, the O_2 binding process is quite different between the two molecules. In hemoglobin, the O_2 dissociation curve shows the so-called S-form due to the allosteric effect, while in myoglobin the O_2 dissociation curve is hyperbolic. In hemoglobin, the present allosteric model proposes that the change of the quarternary structure between T- and R-forms controls the O_2 affinity. The T- and R-forms have low and high oxygen affinity, respectively.[11,12]

The O_2 affinity of myoglobin and hemoglobin has been studied experimentally from mainly two perspectives: with regard to substitution of the amino acid residue[3–5] and substitution of heme itself by a similar modified heme (Fe–porphycene, Fe–azaporphyrinm, etc.).[13–17] The former studies concern the allosteric mechanism of hemoglobin. Hemoglobin has four subunits connected each other by salt bridges, hydrogen bonds, and van der Waals interactions. Although there is no firm conclusion on the allosteric effect, it is known that these interactions control the structure of the active site, heme, in hemoglobin.[11,12] Therefore, it is worth investigating how the structure change affects the O_2 binding. In the latter studies, Hayashi et al. reported that the replacement of heme itself (Fe–porphyrin) by the modified heme (Fe–porphycene) in myoglobin had extremely high O_2 affinity (compared to the native myoglobin, more than 1000 times).[16,17] This result shows that the electronic structure of the active site itself, is very important in the O_2 affinity. Therefore, quantum mechanical calculation on the active site could draw important conclusion.

The electronic structures of oxyheme and deoxyheme have been theoretically studied at several theoretical levels, MNDO/d,[18] QM/MM,[19–21] DFT using LSD schemes,[22–24] CASSCF,[25–27] CASPT2,[28] and SAC/SAC-CI[29] calculations.[30] These studies mainly addressed the electronic structures of oxyheme and deoxyheme but not the change in the electronic structure during the O_2 binding process. In this study, we focus the O_2 binding process. The electronic structures of oxyheme and deoxyheme and their stabilities are rather subtle problems, because of the existence of many possible spin states and the electron correlations. Therefore,

Correspondence to: H. Nakatsuji; e-mail: hiroshi@sbchem.kyoto-u.ac.jp

Contract/grant sponsor: the Grant for Creative Scientific Research from the Ministry of Education, Science, Sports and Culture

we will discuss these problems, comparing our calculations with several theoretical studies.

There are two important aspects in the dioxygen binding process in the active site of myoglobin and hemoglobin: the change in the spin state and the change in the structure of heme.[31] Intersystem crossing is necessary in the O_2 binding process. The ground states of deoxyheme and O_2 molecule are in quintet (S = 2) and triplet state (S = 1), respectively, and the total system is triplet. In oxyheme, the spin multiplicity becomes low-spin singlet state (S = 0) after the O_2 binding.[32,33] A large structural change is also seen in the O_2 binding process. Oxyheme has the Fe atom in the same plane as the porphyrin ring, while there are large deviations from the plane in the deoxyheme (myoglobin: 0.3–0.4 Å, hemoglobin: 0.5–0.6 Å).[34–38]

In this study, we investigated these two aspects that could be important in the reversible O_2 binding process in myoglobin and hemoglobin. We studied the electronic structure of oxy-/deoxyheme and the potential energy surface for the O_2 binding process using the Density Functional Theory to understand how these factors control the oxygen affinity.

Computational Details

We studied model systems: O_2–Fe(II)–Porphin(Por)–Imidazole(Im) for oxyheme and Fe(II)–Por–Im for deoxyheme (Fig. 1). DFT (UB3LYP) calculations were performed with the following basis set and geometries using the Gaussian98 program package.[39] The basis set used was 6-31g* for Fe, O, and pyrrole N atoms and 6-31g for the other atoms.[40]

To identify the spin-multiplicity of the ground state, we determined the energy-minimum structure of deoxyheme in singlet, triplet, and quintet states and oxyheme in singlet and triplet states.

Next, we calculated the potential energy surfaces of the O_2 binding process in the singlet and triplet states as functions of two reaction coordinates: d (the deviation of the Fe atom from the porphyrin plane) and the distance R between Fe and O_2 (Fig. 1). We selected 46 points that were placed at intervals of 0.1 Å for coordinate d and at intervals of 0.2 Å (or 0.1 Å near minimal point) about coordinate R. In this calculation, other atomic coordinates except for d and R were changed linearly between the optimized geometry for the singlet state of oxyheme (O_2-binding state) and that for the triplet state of oxyheme (dissociation limit). We first optimized the atomic coordinates for O_2-binding state (X_{bind}) and dissociation limit (X_{dis}). With a parameter λ ($0 \leq \lambda \leq 1$), the atomic coordinates between the two structures were linearly defined as eq. (1). At each point, the Fe–O_2 distance, R, was changed, keeping all other geometric parameters fixed.

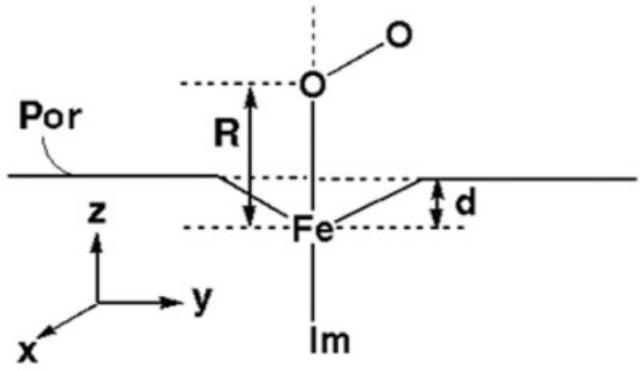

Figure 1. Illustration of the calculation model. Two reaction coordinates are defined: d (Å) (the deviation of Fe from the porphyrin plane) and R (Å) (the distance between Fe and dioxygen). In this figure, "Im" means imidazole and "por" means porphyrin ring.

$$X = \lambda X_{bind} + (1 - \lambda) X_{dis} . \quad (1)$$

Table 1. Optimized Geometries and Total Energies of Deoxyheme and Oxyheme in Several Spin States.

	Deoxyheme			Oxyheme	
	Quintet[a]	Triplet	Singlet	Triplet	Singlet[b]
Relative energy (kcal/mol)	0.00	0.671	6.48	8.36	0.00
Optimized geometry distance (Å)					
Fe–Im N	2.13 (2.134)	2.21	1.91	2.14	2.07 (2.07)
Fe–Pyr N	2.09 (2.075)	2.01	2.00	2.09	2.01 (1.97–1.99)
Fe–O	—	—	—	2.91	1.85 (1.75)
O–O	—	—	—	1.22	1.29 (1.15–1.32)
Fe–Por plane	0.429 (0.34)	0.190	0.201	0.394	0.0253 (0.03)
angle (degree)					
Pyr N–Fe–Pyr N	88.8	89.1	89.6	89.0	89.6
	88.7	90.4	89.8	88.9	90.7
Pyr N–Fe–Im N	98.6	94.2	94.7	99.1	89.5
Fe–O–O	—	—	—	119.7	118.1 (129–133)
Dihedral angle (degree)					
Pyr N–Fe–Im N–Im C	0.204	44.8	44.9	2.67	44.2

[a]The values in the parenthesis are the X-ray structural data for the biomimetic myoglobin model.[37]
[b]The values in the parenthesis are X-ray structural data for the biomimetic oxymyoglobin model.[38]

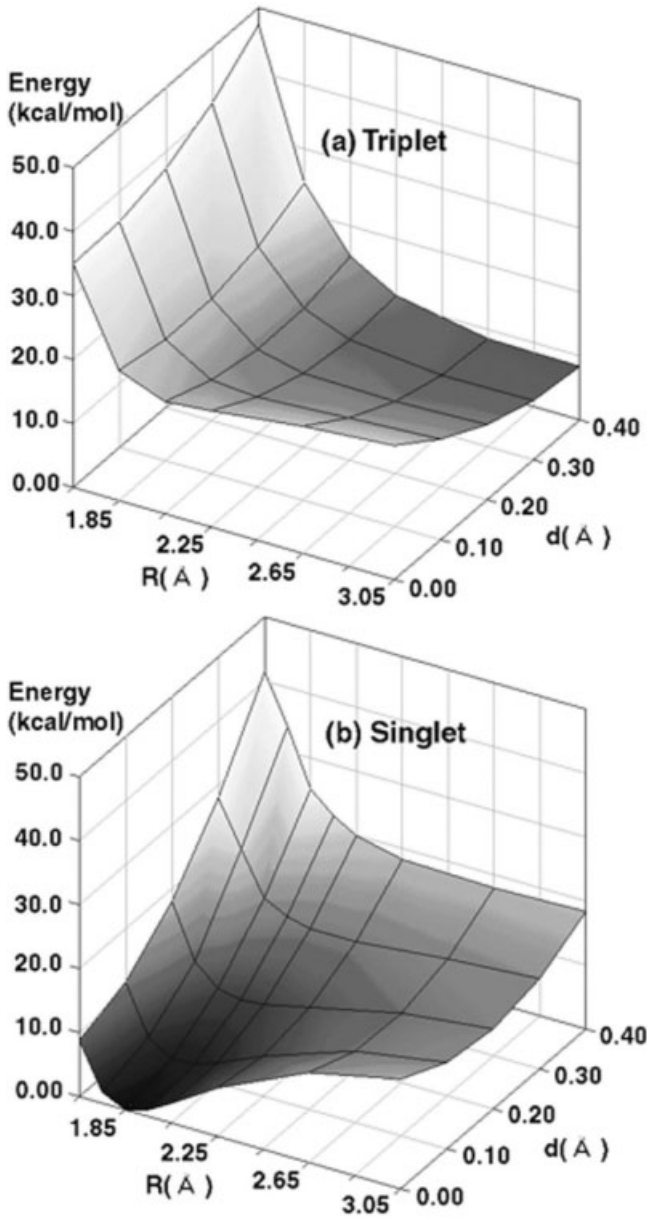

Figure 2. The potential energy surface in each spin state as a function of two reaction coordinates: d (Å) (the deviation of Fe from the porphyrin plane) and R (Å) (the distance between Fe and dioxygen). A darker color shows greater stability.

We later checked the relaxation effects on the potential energy surface and found that the structural relaxation gave only minor changes in the potential surface as described earlier.

Results and Discussion

Ground States of Deoxyheme and Oxyheme

First, we investigated the geometries and electronic structures of the ground state of deoxyheme and oxyheme. Table 1 shows the optimized geometry and relative energy in each spin multiplicity. The ground state of deoxyheme was calculated to be a quintet state, and the triplet and singlet states locate 0.67 kcal/mol and 6.48 kcal/mol higher than the quintet state, respectively. Although the energy difference among these states are very small, the present conclusion agrees with the previous experimental study: in a heme model, Fe(II)–OEP(OctaEthylPorphyrin)–(2-MeIm),[41] and the active sites of myoglobin and hemoglobin protein,[31–33] the ground-state spin-multiplicity is quintet.

The optimized geometry of the quintet state is quite different from those of the triplet and singlet states. In the quintet state, the Fe atom lies out of the porphyrin plane by $d = 0.429$ Å, which is much larger than the cases of the triplet state (0.190 Å) and the singlet state (0.201 Å). The calculated geometry for the quintet state agrees with the results obtained by X-ray crystallographic data for both myoglobin and biomimetic complexes,[34–38] in which this deviation of Fe distributes around 0.3–0.4 Å (0.34 Å for a biomimetic deoxymyoglobin model[37]). The electronic reason of the position of the Fe atom is relevant to the occupation of the $d_{x^2-y^2}$ orbital in the quintet state (the $d_{x^2-y^2}$ orbital is unoccupied in the triplet and singlet states). Because the $d_{x^2-y^2}$ orbital has antibonding interaction with the lone pair of the pyrrole N in the porphyrin plane, the out-of-plane position becomes stable. As shown in Table 1, the dihedral angle, Pyr N–Fe–Im N–Im C, of quintet deoxyheme (0.204°) is different from those of triplet (44.8°) and singlet deoxyheme (44.9°). In the quintet state, the $d_{x^2-y^2}$ orbital interacts with the π orbital of imidazole, and this interaction results in the change of the dihedral angle. The geometrical parameters agree reasonably well with those of a biomimetic deoxymyoglobin model[37] as shown in Table 1.

The ground state of oxyheme is the singlet state, and the triplet state locates 8.36 kcal/mol higher than the singlet state. As shown in Table 1, the optimized geometry of the singlet state is in reasonable agreement with the experimental X-ray crystallographic data for both myoglobin and biomimetic complexes.[34–38] The Fe atom locates inside the porphyrin-plane. The distance between Fe and O_2 was 1.85 Å. The O—O bond length was 1.29 Å, which is very close to free O_2. In the triplet state, the Fe atom lies out of the porphyrin plane by 0.394 Å. The Fe—O and O—O distance is 2.91 and 1.22 Å, respectively. The Fe—O distance of the triplet oxyheme is by 1.0 Å larger than that of the singlet oxyheme. The imidazole plane is parallel to the Fe–pyrrole N plane in contrast to the 45° rotated structure in the singlet state. These results indicate that the electronic structure of the triplet ground state is described as Fe(S = 2) + O_2(S = 1): the electronic

Table 2. O_2 Affinity of Heme in Single and Triplet States and in Different Deviation of the Fe Atom.

Spin multiplicity	Deviation of Fe	Potential curve	Oxygen affinity
Singlet	in plane	Associative	High
Singlet	out of plane	Slightly associative	Very low
Triplet	in plane	Slightly associative	Very low
Triplet	out of plane	Dissociatibve	None

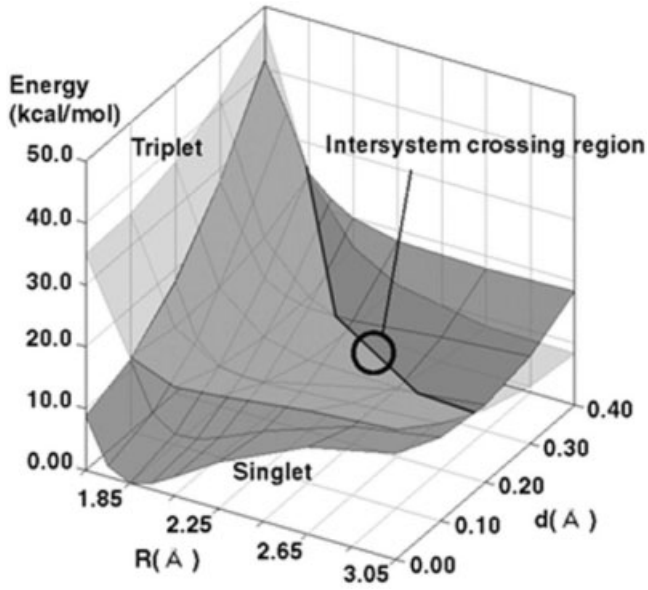

Figure 3. The potential energy surface with the singlet state on the triplet state. A dark color shows the singlet state surface and a bright color shows the triplet state surface. The intersystem crossing area appears at $d = 0.2$–0.3 Å and $R = 2.2$–2.5 Å.

structure of the Fe–Por–Im moiety is very close to that of the quintet state of deoxyheme, Fe(S = 2). Therefore, the triplet state of oxyheme does not bind O_2 strongly, as we see in the next section. Most theoretical and experimental studies suggested that the heme binds O_2 in singlet ground state.[18–24,26,27,29] We will discuss the electronic structure of the O_2 binding state in the next section in more detail.

The Potential Energy Surface for the O_2 Binding Process

We investigated the potential energy surface for the O_2 binding process in triplet and singlet states as functions of d and R (see Fig. 1) to understand the mechanism of the O_2 binding.

As seen in Figure 2a, the potential energy surface of the triplet state is entirely dissociative. In the dissociation limit, the total electronic structure is Fe(S = 2) + O_2(S = 1): the ground states of deoxyheme (quintet state) and O_2 (triplet state). The Fe atom locates the out-of-plane position in the dissociation limit, as in the ground state of deoxyheme. One exception is the case that the parameter d (distance from the porphyrin plane) is fixed to around zero. The potential curve becomes slightly associative, even though the binding energy is very small.

On the other hand, the potential energy surface of the singlet state is entirely associative. In the energy minimal structure, the Fe atom locates in the porphyrin plane. We also found that the character of the potential curve depends on the parameter d. With the Fe atom fixed around the porphyrin plane ($d \approx 0.0$) the potential curve is highly associative, while the curve becomes dissociative when the Fe atom is fixed at out of the plane.

As explained earlier, the structural parameters except for R and d were linearly changed between the binding structure and the dissociation limit in calculating the potential energy surfaces. We describe here the effect of the structural relaxation to the potential surfaces. To confirm the results shown in Figure 2, we carried out geometry optimization with fixed R and d at structures (1) near to O_2 binding state (small R and small d), (2) near the dissociation limit (large R and large d), and (3) intermediate between them (middle R and middle d). First, there was no crucial difference between the partially optimized and linearly changed structures in all cases (1–3). Second, the error in the potential surfaces due to the lack of the structure relaxation is expected to be at most 1 kcal/mol. Because we performed the optimization of all structural parameters for both the binding state and dissociation limit, the linearly changed structures around (1) and (2) would be reliable. For the structure around (3), the energy change due to the relaxation was calculated to be 1.08 kcal/mol in the singlet state, which was the worst example in the examinations.

Thus, two important conclusions are derived: (1) Heme binds O_2 only in its singlet state, because the potential surface is entirely associative. (2) The potential curve becomes associative when the Fe atom locates close to the porphyrin plane, while the potential curve changes into dissociative when the Fe atom lies out of the plane. The former indicates the importance of the relativistic effect, spin-orbit interaction, in the O_2 binding. The latter indicates that the O_2 affinity can be controlled by tuning the geometry parameter d, the deviation of the Fe atom from the porphyrin ring. Table 2 summarizes the oxygen affinity in terms of the spin multiplicity and the deviation of the Fe atom.

The Electronic Structure and the O_2 Affinity

The O_2 affinity is mainly controlled by (1) the spin multiplicity of the oxyheme and (2) the deviation of the Fe atom from the porphyrin plane. We analyze these results from the electronic structural view point.

Spin State

As shown in Table 2, oxyheme has high O_2 affinity only in the singlet state. In the triplet state of oxyheme, an unpaired electron occupies the Fe($d_{x^2-y^2}$) orbital, while the electron is in the Fe(d_{yz}) orbital as paired electron in the singlet state. This would be one reason of the difference in the O_2 affinity between the triplet and singlet states. Because the Fe($d_{x^2-y^2}$) orbital and the N(lone pair) of pyrrole have antibonding interaction, the Fe atom prefers to be out of the porphyrin plane. Thus, the electronic structure of the Fe–Por–Im moiety is very similar to that of deoxyheme in the quintet state.

Deviation of the Fe Atom from the Porphyrin Plane

Because the Fe(d_{z^2}) orbital forms an s-bond with the $O_2(\pi^*)$ orbital, this orbital could be related to the dependency between the O_2 affinity and the position of the Fe atom. When the Fe atom locates in-plane, the Fe(d_{z^2}) orbital cannot interact with the π orbitals of the porphyrin ring due to symmetry. However, when the Fe atom locates out of plane, the Fe(d_{z^2}) orbital can interact with the π orbital of the porphyrin ring due to the broken symmetry. This makes the Fe(d_{z^2}) orbital stable because π-electron of the

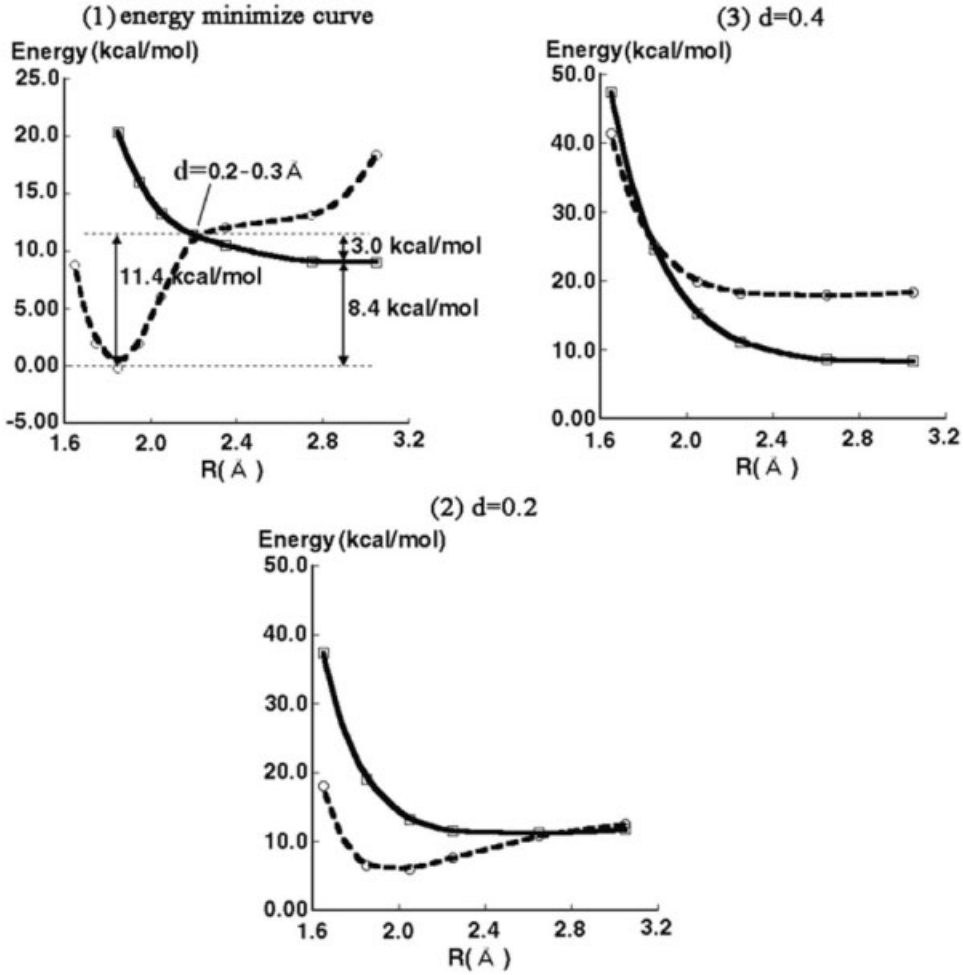

Figure 4. The one-dimensional potential energy curve for the O_2 binding for the singlet (the dotted line) and triplet (the solid line). (1) Approximate energy-minimum potential curve extracted from Figure 3. The intersystem crossing occurs around d = 0.2–0.4 Å. (2, 3) The cross-section view of the Figure 3 at d = 0.2 (2) and d =0.4 (3).

porphyrin flows into the Fe(d_{z^2}) orbital. Therefore, the interaction between the Fe(d_{z^2}) and the O_2(π*) orbitals becomes weaker.

Intersystem Crossing in the O_2 Binding Process

In Figure 3, the singlet and triplet potential surfaces were compared. The ground state of oxyheme is singlet in the binding region, while the triplet state is the ground state in the dissociation limit. In addition, the potential surface of the triplet state is entirely dissociative. Therefore, intersystem crossing is indispensable in the O_2 binding process. The interaction that allows the crossing is the spin–orbit interaction. In this sense, relativistic effect is essentially important for the O_2 binding in the living bodies.

Next, we analyze the potential energy surface with the singlet state upon the triplet state, as shown in Figure 3. There is a region where the intersystem crossing occurs. Because the energy levels of single and triplet states become degenerate in this region, the spin conversion is expected to happen easily, even though the spin–orbit interaction is very small. The area of the crossing appears in the range d = 0.2–0.4 Å, and there is no crossing in d = 0.0–0.1 Å. Because the O_2 actual binding process occurs approximately along the energy-minimum pathway, the actual intersystemcrossing area would be around d = 0.2–0.3 Å and R = 2.2–2.5 Å.

On the Reversible O_2 Binding

To understand the O_2 binding process, we extract energy-minimal O_2 binging pathway from Figure 3. As seen in Figure 4a, starting with the dissociation limit, the system in triplet state reaches to the intersystem crossing point by climbing over an energy barrier of 3.0 kcal/mol. At the crossing point, the triplet state converts into the singlet state due to the spin–orbit interaction. The system then proceeds to the O_2 binding state on the singlet potential energy surface. Consequently, the system gains 8.4 kcal/mol of the binding energy. In the O_2 dissociation, the system in singlet state needs 11.4 kcal/mol to reach the intersystem

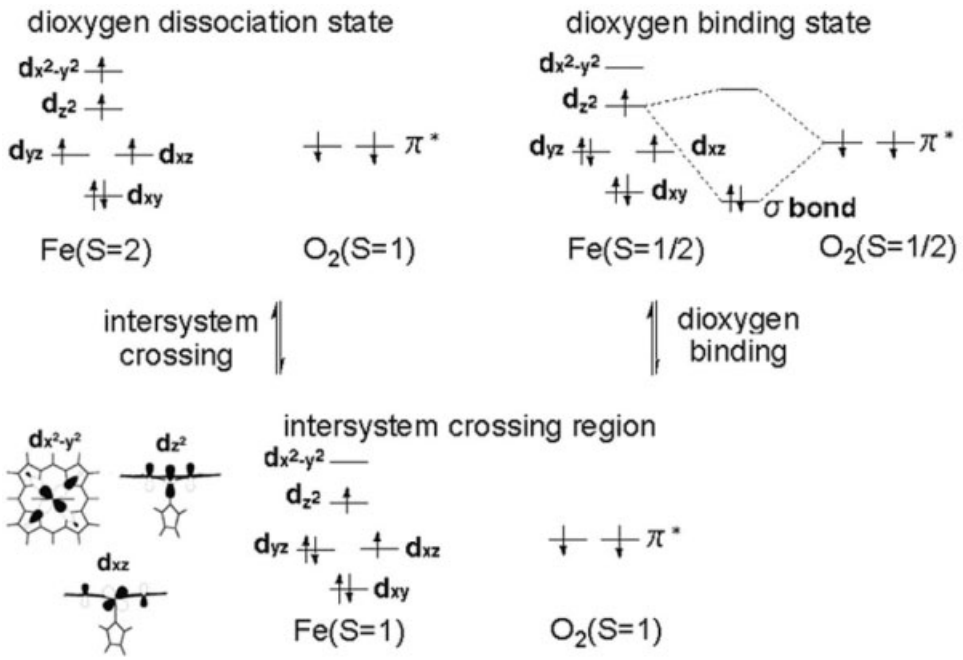

Figure 5. The $d_{x^2-y^2}$, d_{z^2}, and d_{xz} orbitals, and the change in electronic structure upon dioxygen binding.

crossing region. After the spin state changes into the triplet state, oxyheme releases O_2 and reaches to the dissociation limit. If the O_2 binding occurs only along the singlet surface, the activation energy would be approximately 20 kcal/mol, which makes the O_2 release process very difficult. In this sense, the relativistic effect plays an important role in the reversible O_2 binding.

Using the calculated potential surface, we estimated the equilibrium constant for the O_2 binding and compared it with that of human myoglobin. Our result shown in Figure 4a might be close to the situation in human myoglobin, because myoglobin does not show the allosteric effect.

$$K = e^{\frac{\Delta G}{RT}} \approx e^{\frac{\Delta E}{RT}}. \qquad (2)$$

In eq. (2), we assume that the entropy effects are constant and estimate the equilibrium constant from the binding energy (ΔE) instead of free energy (ΔG). The theoretically estimated equilibrium constant obtained from eq. (2) was 1.8×10^6 [M^{-1}] at 20°C. The experimental value obtained for human myoglobin protein is 1.1×10^6 [M^{-1}] at pH 7.0 and 20°C.[42] Although we did not consider the effects of the surrounding protein, the estimated equilibrium constant is close to the experimental value. This may indicate that the interaction between heme and O_2 dominates the binding process more than that with the surrounding protein residues.

Next we examined a situation where an external confinement restricts the geometry: An external force acts on the imidazole, and the Fe atom moves out of the porphyrin ring. This was mimicked

Table 3. Spin Population of Oxyheme in the O_2 Binding State, the Crossing Region, and the O_2 Dissociation Limit.

	O_2 binding state (singlet)	Crossing region (d = 0.2, R = 2.25) (singlet)	O_2 dissociation limit (triplet)
Gross orbital spin population:			
$d_{x^2-y^2}$	0.0733	0.1792	0.7992
d_{z^2}	0.1306	0.4958	0.8025
d_{yz}	0.4386	0.3470	0.9454
d_{xz}	0.4368	0.6234	0.9281
d_{xy}	0.0288	0.0519	0.1123
Atomic spin population:			
Fe	1.1520	1.7703	3.8825
O_2	−1.0864	−1.6933	−1.9944

with the fixed parameter d. Figure 4b and c shows the cross-section view of Figure 3 at $d = 0.2$ and 0.4 Å, respectively. In the case of $d = 0.2$ Å, the valley of the singlet-state potential curve becomes shallow, while there is little change in the triplet-state potential curve. The activation energy for the O_2 dissociation significantly decreased to about 5 kcal/mol. Approximately 6 kcal/mol of energy should be used for pulling the Fe–Imidazole moiety toward outside. In the case of $d = 0.4$ Å, the potential curve for the singlet states turns to dissociative, while the triple state shows only minor change in the potential curve. There is almost no energy barrier to dissociate O_2 molecule.

In summary, owing to the relativistic effect, the spin–orbit interaction in this case, heme obtains high reversibility in the O_2 binding. When heme is free from the structural confinement by the protein environment, it is natural for the system to go along the energy-minimal pathway and to bind O_2 with the activation barrier of only 3.0 kcal/mol, as shown in Figure 4a. Change of the structural parameter d from in-plane to out-of-plane significantly switches the singlet-state potential curve from associative to disscociativey. When one assumes that heme has an external confinement forcing the Fe–Imidazole unit to be out of the porphyrin ring, oxyheme easily releases O_2 molecule without large activation energy.

The Electronic Structure of Oxyheme and Its Changes during the O_2 Binding

In this section, we describe the electronic structure of oxyheme in the O_2 binding process. Figure 5 illustrates the changes of the electronic structure. Table 3 shows the spin population on each orbital and on each atom. In the O_2 dissociation limit, the spin multiplicity is triplet: heme and O_2 are in quintet ($S = 2$) and triplet ($S = 1$) states, respectively (Mulliken spin population: Fe:3.8825, O_2: −1.9944).

The O_2 molecule approaches to the intersystem crossing point, and the spin multiplicity converts into the singlet state. In this transition, an electron in the $d_{x^2-y^2}$ orbital flips its spin state and moves to the d_{yz} orbital. This is seen in Table 3. The spin population of the $d_{x^2-y^2}$ orbital 0.80 decreases to 0.18 and, that of the d_{yz} orbital 0.95 decreases to 0.35. The O_2 molecule is still has two unpaired electron in this structure (spin population on Fe and O_2 is 1.77 and −1.69, respectively).

Finally, the O_2 molecule reaches to the binding state. Heme forms a σ-bond between the Fe(d_{z^2}) orbital and $O_2(\pi^{*,\parallel})$ orbital, where $\pi^{*,\parallel}$ denotes the π^* orbital parallel to the mirror plane (yz plane) of the molecule. In the binding state, there is no apparent π-bond (π-back donation) between the Fe atom and O_2 molecule. As shown in Figure 5, the ground state of oxyheme is an open-shell singlet state: a biradical state having unpaired elections in each Fe(d_{xz}) and $O_2(\pi^{*,\perp})$ orbitals (Mulliken spin population: Fe:1.15, O_2: −1.09). The $\pi^{*,\perp}$ orbital denotes π^* orbital perpendicular to the mirror plane (yz plane) of the molecule. These two orbitals show little interaction each other, not like the ground state of O_3 molecule (a biradical electronic structure with singlet coupling). Therefore, the electronic structure in the ground state of oxyheme is different from Goddard model[43] and characterized as s-bonding between Fe(d_{z^2}) orbital and $O_2(\pi^{*,\parallel})$ and noninteracting unpaired electrons in Fe(d_{xz}) and $O_2(\pi^{*,\perp})$ orbitals. The present result is compared with the previous studies. The DFT studies using LSD schemes also suggested an open-shell singlet ground state,[22–24] which is the same as our results. In contrast, the CASSCF study and the SAC/SAC-CI study suggested that the Hartree–Fock configuration is the main configuration in the ground state, although the weight of the Hartree–Fock configuration was rather small. These results indicates that these strong configuration interaction describes the biradical electronic structure.[26,27,29] Fe(d_{xz}) and Fe(d_{yz}) orbitals are almost equivalent by the symmetry reason. However, Fe(d_{yz}) orbital is slightly lower than Fe(d_{xz}) orbital by the effect of imidazole and Fe—O_2 plane. Therefore, the state in which the Fe(d_{yz}) orbital is occupied by two electrons is more stable than that the Fe(d_{xz}) orbital occupied by two electrons.

We examined the S^2 values of the calculated wave functions. In deoxyheme, the S^2 values of the quintet, triplet and singlet states were 6.0, 2.1, and 0.0, respectively. These values are pure spin multiplicities in each spin state. In oxyheme, these values of the O_2 dissociation limit [triplet: Fe($S = 2$) + O_2 ($S = 1$)] and the O_2 binding state [singlet: Fe($S = 1/2$) + O_2 ($S = 1/2$)] were 4.0 and 0.9, respectively. In the O_2 dissociation limit (triplet), the triplet and higher spin state (septet) are degenerate. The S^2 value: 4.0 is the just median of the values of these two states (triplet : 2.0, septet : 6.0). In the O_2 binding state, as mentioned above, the noninteracting unpaired electrons are left in Fe(d_{xz}) and $O_2(\pi^{*,\perp})$ orbitals. Therefore, the singlet and higher spin state (triplet) are almost degenerate. The S^2 value: 0.9 is also the middle of these two states (singlet: 0.0, triplet: 2.0) the same as in the O_2 dissociation limit. This is the drawback of the single-determinant description for the biradical states. Even though the optimized structures agree well with the X-ray ones, more advanced method should be necessary to confirm the potential surfaces.

Conclusion

We investigated the mechanism of the reversible O_2 binding in heme by using Density Functional Theoretical calculations. First, we optimized the geometries of deoxyheme and oxyheme in their spin-multiplicities to determine the ground state. In deoxyheme, the ground state is the quintet state where the Fe atom deviates greatly from the porphyrin plane. In oxyheme, the ground state is the singlet state where the Fe atom locates in the porphyrin plane. These results are in good agreement with experimental findings. These facts indicate that the electronic structure of the active site (heme) controls the geometry (planarity), rather than the surrounding protein effects.

Next, we studied the potential energy surfaces as functions of the deviation of the Fe atom from the porphyrin ring and the Fe–O_2 distance. The results indicate that the potential energy surface is entirely associative in singlet state, while it is dissociative in triplet state. The potential curve becomes associative when the Fe atom locates close to the porphyrin plane, while the potential curve changes into dissociative when the Fe atom lies out of the plane. This is because the large deviation of the Fe atom prevents σ bond formation between the Fe atom and O_2 molecule. Comparing the potential energy surfaces of the singlet and triplet states, we found the intersystem crossing area (d: 0.2–0.3 Å, R: 2.2–2.5 Å), where the singlet and triplet states accidentally degenerate. Thus, the O_2 binding process proceeds from the triplet to the singlet states due

to the spin–orbit interaction. We applied the present potential surface to estimate the equilibrium constant. The calculated 1.8×10^6 [M^{-1}] is close to the experimental value 1.1×10^6[M^{-1}], indicating that the O_2 affinity is controlled by the electronic structure of oxyheme rather than the surrounding protein effects.

The transition probability by spin–orbit interaction is generally expected to be not as large. However, for the living bodies to survive, the intersystem crossing should be easily accomplished. Therefore, the O_2 binding reaction pathway should be firm and stable. It would be interesting to say that the relativistic effect works every time when we breathe.

We also studied the potential curve of the O_2 binding with the parameter d fixed to 0.2 and 0.4 Å. Although the triplet state was insensitive to the parameter d, the singlet state shows significant changes in the potential curve. With the larger d, the potential curve becomes shallower. At $d = 0.4$ Å, the potential curve becomes dissociative. These results indicate that the change of d, the deviation of the Fe atom from the porphyrin ring, would be important reaction coordinate which controls the O_2 affinity.

Change of the electronic structure during the binding process was also studied. In the O_2 dissociation limit, the whole system in the triplet state includes heme in the quintet state and dioxygen in the triplet state. When O_2 approaches to heme and arrives at the intersystem crossing point, the spin state of the system changes from the triplet state to the singlet state by the spin–orbit coupling, so the spin state of heme moiety becomes the triplet state. The Fe(d_{xz}) and Fe(d_{z^2}) orbitals are SOMO in the triplet state. When the O_2 further approaches to heme and arrives at the O_2 binding state, the σ bond is formed between the Fe(d_{z^2}) orbital of the Fe atom and the O_2 (π^*) orbital of dioxygen, while there is no strong π bond. The electronic structure of O_2 binding state is an open-shell singlet state, namely a biradical state with singlet coupling, in which both the d_{xz} orbital of Fe and the one π^* orbital of dioxygen have nonzero spin density distribution. There is a strong σ bond, but no π bond formed between the d_{xz} orbital of Fe and the π^* orbital of dioxygen. Therefore, the electronic structure of the O_2 binding state is a biradical state with noninteracting singlet coupling, which is different from that of ozone.

Acknowledgment

A part of the computations was performed in the Research Center for Computational Science, Okazaki, Japan.

References

1. Bernal, J. D.; Fankuchen, I.; Perutz, M. F. Nature 1938, 141, 523.
2. Monod, J.; Wyman, J.; Changeux, J. P. J Mol Biol 1965, 12, 88.
3. Englander, J. J.; Rumbley, J. N.; Englander, S. W. J Mol Biol 1998, 284, 1707.
4. Bettati, S.; Mozzarelli A.; Perutz, M. F. J Mol Biol 1998, 281, 581.
5. Kim, H. W.; Shen, T. J.; Ho, N. T.; Zou, M.; Tam, M. F.; Ho, C. Biochemistry 1996, 35, 6620.
6. Tokita, Y.; Nakatsuji, H. J Phys Chem B 1997, 101, 3281.
7. Jewsbury, P.; Yamamoto, S.; Minato, T.; Saito, M.; Kitagawa, T. J Phys Chem 1995, 99, 12677.
8. Obara, S.; Kashiwagi, H. J Chem Phys 1982, 77, 3155.
9. Ghosh, A.; Bocian, D. F. J Phys Chem 1996, 100, 6363.
10. Jewsbury, P.; Yamamoto, S.; Minato, T.; Saito, M.; Kitagawa, T. J Am Chem Soc 1994, 116, 11586.
11. Liddington, R.; Derewenda, Z.; Dodson, G.; Harris, D. Nature 1998, 331, 725.
12. Eaton, W. A.; Henry, E. R.; Hofrichter, J.; Mozzarelli, A. Nat Struct Biol 1999, 6, 351.
13. Neya, S.; Kaku, T.; Funasaki, N.; Shiro, Y.; Iizuka, T.; Imai, K.; Hori, H. J Biol Chem 1995, 270, 13118.
14. Neya, S.; Hori, H.; Imai, K.; Kawamura–Konishi, Y.; Suzuki, H.; Shiro, Y.; Iizuka, T.; Funasaki, N. J Biochem 1997, 121, 654.
15. Neya, S.; Tsubaki, M.; Hori, H.; Yonetani, T.; Funasaki, N. Inorg Chem 2001, 40, 1220.
16. Hayashi, T.; Dejima, H.; Matsuo, T.; Sato, H.; Murata, D.; Hisaeda, Y. J Am Chem Soc 2002, 124, 11226.
17. Matsuo, T.; Dejima, H.; Hirota, S.; Murata, D.; Sato, H.; Ikegami, T.; Hori, H.; Hisaeda, Y.; Hayashi, T. J Am Chem Soc 2004, 126, 16007.
18. Taranto, A. G.; Carneiro, J. W. M.; Oliveira, F. G. J Mol Struct (Theochem) 2001, 539, 267.
19. Marechal, J.; Barea, G.; Maseras, F.; Lledos, A.; Mouawad, L.; Perahia, D. J Comput Chem 2000, 21, 282.
20. Maseras, F. New J Chem 1998, 327.
21. Barea, G.; Maseras, F.; Lledos, A. Int J Quantum Chem 2001, 85, 100.
22. Rovira, C.; Kunc, K.; Hutter, J.; Ballone, P.; Parrinello, M. Int J Quantum Chem 1998, 69, 31.
23. Rovira, C.; Parrinello, M. Int J Quantum Chem 1998, 70, 387.
24. Rovira, C.; Parrinello, M. Int J Quantum Chem 2000, 80, 1172.
25. Choe, Y.; Hashimoto, T.; Nakano, H.; Hirao, K. Chem Phys Lett 1998, 295, 380.
26. Yamamoto, S.; Kashiwagi, H. Chem Phys Lett 1989, 161, 85.
27. Yamamoto, S.; Kashiwagi, H. Chem Phys Lett 1993, 205, 306.
28. Choe, Y.; Nakajima, T.; Hirao, K.; Lindh, R. J Chem Phys 1999, 111, 3837.
29. Nakatsuji, H.; Hasegawa, J.; Ueda, H.; Hada, M. Chem Phys Lett 1996, 250, 379.
30. Bytheway, I.; Hall, M. B. Chem Rev 1994, 94, 639.
31. Scheidt, W. R.; Reed, C. A. Chem Rev 1981, 81, 543.
32. Pauling, L.; Coryell, C. N. Proc Natl Acad Sci USA 1936, 22, 210.
33. Montenteau, M.; Reed, C. A. Chem Rev 1994, 94, 659.
34. Phillips, S. E. V. Nature 1978, 273, 247.
35. Phillips, S. E. V. J Mol Biol 1980, 142, 531.
36. Fermi, G. J Mol Biol 1975, 97, 237.
37. Momenteau, M.; Scheidt, W. R.; Eigenbrot, C. W.; Reed, C. A. J Am Chem Soc 1988, 110, 1207.
38. Jameson, G. M.; Rodley, G. A.; Robinson, W. T.; Gagne, R. R.; Reed, C. A.; Collman, J. P. Inorg Chem 1978, 17, 850.
39. Frisch, M. J.; Trucks, G. W.; Schlegel, H. B.; Scuseria, G. E.; Robb, M. A.; Cheeseman, J. R.; Strain, M. C.; Burant, J. C.; Stratmann, R. E.; Dapprich, S.; Kudin, K. N.; Millam, J. M.; Daniels, A. D.; Petersson, G. A.; Montgomery, J. A.; Zakrzewski, V. G.; Raghavachari, K.; Ayala, P. Y.; Cui, Q.; Morokuma, K.; Foresman, J. B.; Cioslowski, J.; Ortiz, J. V.; Barone, V.; Stefanov, B. B.; Liu, G.; Liashenko, A.; Piskorz, P.; Chen, W.; Wong, M. W.; Andres, J. L.; Replogle, E. S.; Gomperts, R.; Martin, R. L.; Fox, D. J.; Keith, T.; AlLaham, M. A.; Nanayakkara, A.; Challacombe, M.; Peng, C. Y.; Stewart, J. P.; Gonzalez, C.; Head–Gordon, M.; Gill, P. M. W.; Johnson, B. G.; Pople, J. A. Gaussian98; Gaussian Inc.: Pittsburgh, PA, 1998.
40. Hariharan, P. C.; Pople, J. A. Theoret Chim Acta 1973, 28, 213.
41. Kitagawa, T.; Teraoka, J. Chem Phys Lett 1979, 63, 443.
42. Springer, B. A.; Sligar, S. G.; Olson, J. S.; Phillips, G. N., Jr. Chem Rev 1994, 94, 699.
43. Goddard, W. A., III; Olasfson, B. D. Proc Natl Acad Sci US 1975, 72, 2335.